Journal of Experimental Botany, Vol. 70, No. 21 pp. 6349–6361, 2019
doi:10.1093/jxb/erz367 Advance Access Publication August 17, 2019
This paper is available online free of all access charges (see https://academic.oup.com/jxb/pages/openaccess for further details)

RESEARCH PAPER

GABA operates upstream of H$^+$-ATPase and improves salinity tolerance in Arabidopsis by enabling cytosolic K$^+$ retention and Na$^+$ exclusion

Nana Su[1,2,*], Qi Wu[2,3,*], Jiahui Chen[1], Lana Shabala[2], Axel Mithöfer[4], Haiyang Wang[2], Mei Qu[2], Min Yu[3], Jin Cui[1,†] and Sergey Shabala[2,3,†]

[1] College of Life Sciences, Nanjing Agricultural University, Nanjing 210095, China
[2] Tasmanian Institute for Agriculture, College of Science and Engineering, University of Tasmania, Hobart, Tasmania 7001, Australia
[3] International Research Centre for Environmental Membrane Biology, Foshan University, Foshan 528000, China
[4] Research Group of Plant Defense Physiology, Max Planck Institute for Chemical Ecology, D-07745 Jena, Germany

* These authors contributed equally to this work.

† Correspondence: sergey.shabala@utas.edu.au or cuijin@njau.edu.cn

Received 28 September 2018; Editorial decision 30 July 2019; Accepted 2 August 2019

Editor: Ramanjulu Sunkar, Oklahoma State University, USA

Abstract

The non-protein amino acid γ-aminobutyric acid (GABA) rapidly accumulates in plant tissues in response to salinity. However, the physiological rationale for this elevation remains elusive. This study compared electrophysiological and whole-plant responses of salt-treated Arabidopsis mutants *pop2-5* and *gad1,2*, which have different abilities to accumulate GABA. The *pop2-5* mutant, which was able to overaccumulate GABA in its roots, showed a salt-tolerant phenotype. On the contrary, the *gad1,2* mutant, lacking the ability to convert glutamate to GABA, showed oversensitivity to salinity. The greater salinity tolerance of the *pop2-5* line was explained by: (i) the role of GABA in stress-induced activation of H$^+$-ATPase, thus leading to better membrane potential maintenance and reduced stress-induced K$^+$ leak from roots; (ii) reduced rates of net Na$^+$ uptake; (iii) higher expression of *SOS1* and *NHX1* genes in the leaves, which contributed to reducing Na$^+$ concentration in the cytoplasm by excluding Na$^+$ to apoplast and sequestering Na$^+$ in the vacuoles; (iv) a lower rate of H_2O_2 production and reduced reactive oxygen species-inducible K$^+$ efflux from root epidermis; and (v) better K$^+$ retention in the shoot associated with the lower expression level of GORK channels in plant leaves.

Keywords: Arabidopsis, H$^+$-ATPase, hydrogen peroxide, potassium retention, reactive oxygen species, sodium sequestration.

Introduction

Soil salinization affects ~10% of the land surface (950 million ha) and costs agriculture over $27 bn per annum in lost opportunities; this problem is expected to be exacerbated by the current climate changes. As most crop species are sensitive to salt, breeding for salt tolerance remains one of the current priorities of plant breeders. To illustrate this point, the number of published papers having keywords 'salinity stress' and 'breeding' has increased from just four to five per year in early 1990 to 35–40 per year in mid-2000 and exceeded a 150 papers threshold in 2017 (Web of Science data). This reflects the alarming trend in developing soil salinity, which takes about 3 ha of arable land out of production every minute (Shabala

et al., 2014). However, progress in crop breeding for salinity tolerance has been disappointingly slow, and all attempts to improve crop tolerance by targeting salt exclusion traits have not resulted in creating salt-tolerant cultivars for farmers' fields (Shabala, 2013; Ismail and Horie, 2017). This implies that traits other than Na^+ exclusion should be explored in more details. It has also become apparent that it is the mode of regulation of various ion transporters and their upstream signaling, rather than the molecular identity of transporters *per se*, that is critical to confer salinity stress tolerance.

γ-Aminobutyric acid (GABA) is a four-carbon non-proteinogenic amino acid that was first isolated from potato tubers over half a century ago (Steward *et al.*, 1949). In animals, GABA acts as an inhibitory neurotransmitter and also as a signaling molecule; this role has been extensively studied over the last six decades. In plants, the evidence has been mounting since the 1990s that GABA may also act as a signaling molecule (Ramesh *et al.*, 2017), besides being a defensive compound against insect herbivory (Scholz *et al.*, 2015). GABA is metabolized via a short pathway known as the GABA shunt, in which it is mainly synthesized by the irreversible reaction of the cytosolic enzyme glutamate decarboxylase (GAD; EC 4.1.1.15) using glutamate as a substrate (Fait *et al.*, 2008). GABA catabolism occurs in the mitochondrial matrix of multicellular organisms by the action of GABA transaminase (GABA-T; EC 2.6.1.19) to produce succinic semi-aldehyde (Shelp *et al.*, 2012). The GABA-T encoding gene (*At3g22200*) is present as a single copy in the Arabidopsis genome and was initially termed *pollen–pistil incompatibility 2 (POP2*; Palanivelu *et al.*, 2003).

Variability and a large, rapid increase in GABA concentration in plant tissue (0.02 to 4 μmol g^{-1} FW) is one of the main pieces of evidence that GABA acts as a signal in plants (Ramesh *et al.*, 2017). A multitude of abiotic stresses can drive GABA accumulation in plants, including salinity, oxidative stress, hypoxia, extreme temperature, drought, and waterlogging (Ramesh *et al.*, 2015). Of these, the important role of GABA in plant adaptive responses to hypoxia and flooding has received major attention (Miyashita and Good, 2008). Salt-induced GABA accumulation has been also observed broadly in a the number of plant species, including alfalfa, Arabidopsis, barley, tobacco, and soybean (Widodo *et al.*, 2009; Renault *et al.*, 2010; Zhang *et al.*, 2011). The Arabidopsis seedlings produced approximately 20-fold higher GABA under 150 mM NaCl (Renault *et al.*, 2010). Central carbon metabolism and cell-wall modification were changed in an Arabidopsis GABA-T knockout mutant (*pop2*) under salt stress (Renault *et al.*, 2013). Public data from AtGenExpress (http://atpbsmd.yokohama-cu.ac.jp) show that *POP2* transcription in Arabidopsis shoot is up-regulated by 24 h of salt stress, and expression of *GAD* in cells of root stele, root cortex, and root epidermis is down-regulated by 140 mM NaCl at 8 and 48 h. However, it remains unclear whether these changes in GABA levels are essential for plants to deal with salt load, or whether they are merely 'physiological noise', e.g. a by-product of some adaptive responses. To the best of our knowledge, no causal link between salt stress-induced GABA accumulation and activity of key cellular transporters mediating plant ionic homeostasis and metabolism under saline conditions has been reported in the literature.

In Arabidopsis, the *pop2* mutant is unable to produce a functional GABA-T enzyme (Van Cauwenberghe *et al.*, 2002), which leads to the inhibition of GABA degradation, and, as a consequence, causes more GABA accumulation. On the contrary, disruption of the *GAD* gene prevented the accumulation of GABA, because GAD1 and GAD2 play a major role in GABA synthesis in plants (Bouché *et al.*, 2004; Scholz *et al.*, 2015). In this study, we used Arabidopsis *gad1,2* double mutant and *pop2-5* mutant lines to investigate the role of GABA in plant adaptive responses to salinity and its control over the activity of key plasma membrane transporters mediating Na^+ and K^+ homeostasis in plant roots and the modes of their operation. Our work provides a mechanistic explanation for the role of GABA operating upstream of K^+ and Na^+ transporters thus mediating salt-related adaptive responses, and also provides valuable information for improving crop salt tolerance by genetic engineering.

Materials and methods

Plant materials and growth conditions

Arabidopsis Columbia-0 (Col-0) was used as wild-type (WT). Seeds of *gad1,2* and *pop2-5* mutants were kindly provided by Frank Ludewig (University of Erlangen-Nuremberg, Germany). Seeds were surface-sterilized by 20% commercial bleach (1% (v/v) NaClO) for 10 min and thoroughly washed with sterilized distilled water. Seeds were then sown in Petri dishes containing 1% (w/v) phytogel, half-strength Murashige and Skoog (MS) medium, and 0.5% (w/v) sucrose at pH 5.7–5.8, sealed with 3 M micro-pore tape (3M Health Care, St Paul, MN, USA). After 2 d of stratification at 4 °C, Petri dishes were placed in a growth chamber and positioned vertically to allow root growth along the surface of the medium. The conditions in the growth chamber were 16 h/8 h light/dark cycles, with 100 μmol m^{-2} s^{-1} photon flux density during the light period, and temperature at 22 °C. Unless specified, all chemicals were of analytical grade from Sigma-Aldrich (Castle Hill, NSW, Australia). The relative expression of *GAD1–GAD5* and *POP2* genes in plant roots was measured to demonstrate that mutant lines used are true knockout (see Supplementary Fig. S1 at *JXB* online). In some experiments, two additional mutant lines—*pop2* (CS415022, T-DNA insertion, https://www.arabidopsis.org/servlets/TairObject?type=germplasm&id=6530372490; GABA overaccumulating) and *gad1* (SALK_017810, T-DNA insertion, https://www.arabidopsis.org/servlet/TairObject?id=230900&type=stock; with reduced GABA production ability)—were used to validate most critical conclusions made. Their homozygosis was shown (Supplementary Fig. S2). These seeds were kindly provided by Alberto Macho (Shanghai Center for Plant Stress Biology, Chinese Academy of Sciences, China).

Whole-plant physiological assessment

Two types of phenotyping experiments were conducted, for plants grown on either soil or agar medium. In the latter case, surface-sterilized seeds were sown in Petri dishes in 1/2 strength MS medium containing appropriate salt concentration (0, 50, 100, and 150 mM NaCl). After 2 d of vernalization at 4 °C, Petri dishes were placed in a growth chamber as described above. For root length measurements, Petri dishes were oriented vertically, and plants were grown for 1 week. To determine the shoot fresh weight, Petri dishes were placed horizontally, and plants were allowed to grow for 3 weeks. For pot phenotyping experiments, seeds were sown in 0.2-liter pots filled with peat moss, perlite, vermiculite, and coarse sand (2:1:1:1, v/v), and grown for 4 weeks at 21 °C using a 12/12 h light (photosynthetically active radiation 100 μmol m^{-2} s^{-1})/dark regime. Seedlings were then treated with either 50 or 100 mM NaCl for another 2 weeks added with irrigation on a daily basis. The fresh and dry weight of each plant was then measured. Leaf chlorophyll content was measured using a SPAD meter (SPAD-502, Minolta, Japan). The maximum photochemical efficiency of PSII (chlorophyll fluorescence F_v/F_m ratio)

was measured using an OS-30p chlorophyll fluorometer (Opti-Sciences, USA). All non-distractive measurements were taken on rosette leaves from at least five biological replicates for each treatment in a single experiment.

Leaf sap Na^+ and K^+ content measurement

The Arabidopsis leaves were harvested and quickly frozen in Eppendorf tubes. To measure leaf sap K^+ and Na^+ content, the leaves were thawed and the sap extracted by hand-squeezing the leaf samples as described elsewhere (Cuin *et al.*, 2009). A volume of 50 µl of collected sap was diluted to 5 ml using distilled water and used for the determination of K^+ and Na^+ concentration (in mM) using a flame photometer (Corning 410C, Halstead, UK). Five replicates for each treatment were assessed.

GABA content determination

GABA extraction and quantification was carried out as described previously (Scholz *et al.*, 2017). Briefly, fresh tissue from roots was harvested, frozen in liquid nitrogen and weighed for the determination of GABA content per gram fresh weight. After maceration, GABA was extracted twice with a total volume of 2 ml methanol, and supernatants were combined, dried, and re-suspended in 500 µl methanol. This extract was diluted 1:20 (v/v) with water containing the internal standard (algal amino acid mix ^{13}C, ^{15}N (Isotec, Miamisburg, OH, USA), at a mix concentration of 10 µg ml^{-1}). GABA content was analysed by LC-MS/MS according to Scholz *et al.* (2017) using an API 5000 tandem mass spectrometer (Applied Biosystems, Darmstadt, Germany) operated in positive ionization mode with GABA-specific multiple reaction monitoring to monitor analyte parent ion → product ion—GABA: m/z 104.1→87.1; DP 51, CE 17.

Viability staining

Viability of root cells was assessed 2 h after the salt treatment using fluorescein diacetate (FDA)-propidium iodide (PI) double staining method as described in Koyama *et al.* (1995). FDA (cat. no. F7378; Sigma-Aldrich, St Louis, MO, USA) is permeant through the intact plasma membrane and shows a green color under a fluorescence microscope in viable cells after hydrolysis by the internal esterases (Rotman and Papermaster, 1966). On the other hand, PI (cat. no. P4864; Sigma-Aldrich) is not permeant to live cells, and is commonly used to detect dead cells in a population, showing a red color upon PI–nuclear DNA conjugate formation (Riccardi and Nicoletti, 2006). Accordingly, roots were stained with a freshly prepared 5 g ml^{-1} FDA for 3 min followed by 3 g ml^{-1} PI treatment for 10 min. The double-stained roots were observed under a fluorescence microscope (Leica MZ12; Leica Microsystems, Wetzlar, Germany) illuminated by an ultra-high-pressure mercury lamp (Leica HBO Hg 100 W; Leica Microsystems) and fitted with a Leica I3-wavelength filter cube (Leica Microsystems). The excitation and emission wavelengths were 488/505–530 and 543/585 nm for FDA and PI, respectively. Photographs were taken by a Leica (DFC295; Leica Microsystems) camera fitted on the microscope using image acquisition and processing software LAS V3.8 (Leica Microsystems). During the image acquisition, all the automatic exposure features of the LAS V3.8 were disabled, and exposure time (2.6 s), gain (×2.1), saturation (2.10), and gamma (0.87) were set to constant values as indicated in parentheses for the entire period of the experiment.

Quantification of root viability by TTC method

The 2,3,5-triphenyltetrazolium chloride (TTC) method was used to determine root viability as described elsewhere (Clemensson-Lindell, 1994). This method is based on the existence of a positive correlation between the activity of dehydrogenase in root and the root viability. The dehydrogenase in plant root can reduce TTC to triphenylmethylhydrazone (TTF), which can then be detected by spectrophotometry. Roots (0.2 g) were placed in 10 ml of 0.4% (w/v) TTC in 0.06 mM Na_2HPO_4–KH_2PO_4 solution and vacuum-infiltrated for 15 min. After that, the incubation stood at 37 °C for 10 h. The samples were then extracted in 95% (v/v) ethanol followed by incubation in a water bath at 90 °C for 15 min. The absorbance was recorded at 520 nm.

H_2O_2 production

Two methods were used to compare salinity-stress-induced H_2O_2 production in plant roots. The first method utilized H_2O_2-sensitive fluorescent probe cell-permeant 2′,7′-dichlorodihydrofluorescein diacetate (H_2DCFDA or DCF; Thermo Fisher Scientific, Waltham, MA, USA). The indicator was dissolved in dimethyl sulfoxide (Sigma-Aldrich) to a stock concentration of 1 mM. Then, 20 µM DCF was added to a measuring buffer (10 mM KCl, 5 mM Ca^{2+}-MES, pH 6.1). After 2, 6, 12, and 24 h of NaCl treatment, Arabidopsis seedling roots were incubated in the dye-containing measuring buffers for 30 min in the dark. The stained roots were washed in distilled water for 3 min to remove residual dye before measuring fluorescence intensity in root cells. The fluorescence images of H_2O_2 were collected using excitation at 488 nm and emission at 517–527 nm. Then, fluorescence images were analysed with ImageJ software (NIH, USA) based on integrated density. For each treatment, at least eight biological replicates (individual roots) were measured.

The second (quantitative) method followed the procedure of Hossain *et al.* (2010); 0.5 g fresh roots were ground in 5 ml of 50 mM sodium phosphate buffer (pH 7.8), then centrifuged at ~11 900 *g* for 15 min at 4 °C. The yellow color was developed after reaction of 3 ml supernatant with 1 ml 0.1% $TiCl_4$ containing 20% H_2SO_4 for 10 min at room temperature. The absorbance was then recorded at 410 nm.

Non-invasive ion flux measurements

Net H^+, K^+ and Na^+ fluxes were measured using the non-invasive ion-selective microelectrode ion flux estimation (MIFE) technique (University of Tasmania, Hobart, Australia) as described previously (Shabala and Shabala, 2002; Shabala *et al.*, 2006). Net ion fluxes were calculated using MIFEFLUX software for cylindrical diffusion geometry (Shabala *et al.*, 2006). The principles of MIFE ion flux measurements and all the details of microelectrode fabrication and calibration are available in our previous publications (Shabala *et al.*, 2006). Liquid ionic exchangers used in this work are the commercially available ionophore cocktails.

Prior to the MIFE measurement, 7-day-old Arabidopsis seedlings were immobilized in a 5 ml Perspex measuring chamber (10.5 × 0.8 × 2.0 cm), and 3 ml of basic salt medium (BSM; 0.5 mM KCl + 0.1 mM $CaCl_2$, pH 5.6) was added into the chamber. After 40 min, the net ion fluxes were measured by microelectrodes from either elongation (0.4 mm from the root tip) or mature (5 mm from the root tip) root zone. Steady-state fluxes were measured for 5 min, and then the treatment was applied, followed by another 40 min of measurements. At least 15 replicates were used for each treatment.

Membrane potential measurements

Conventional KCl-filled Ag–AgCl microelectrodes were used for membrane potential measurements in the elongation and mature root zones (Bose *et al.*, 2013). The roots of an intact 7-day-old seedling were immobilized in BSM for 40 min. Resting membrane potential was recorded for 1 min before adding NaCl to the BSM solution. The resulting change in transient membrane potential was continuously monitored for up to 25 min. Membrane potential values of 10 individual seedlings were averaged for each treatment.

RT-qPCR analysis

Total RNA was isolated from root tissues using Trizol extraction reagent (Thermo Fisher Scientific) and the RNA purity was verified by the ratio (>1.9) of 260/280 nm absorbance. DNA-free total RNA (5 g) from different treatments was used for first-strand cDNA synthesis in a 20 µl reaction volume (RevertAid First Strand cDNA Synthesis Kit, Thermo Fisher Scientific) according to the manufacturer's instructions. Real-time quantitative PCR reactions were performed using a Mastercycler® ep realplex real-time PCR system (ABI7500, Thermo Fisher Scientific) with Bestar® Sybr Green qPCR mastermix (DBI Bioscience Inc., Ludwigshafen, Germany) in a 20 µl reaction volume according to the user manual. All primers (see Supplementary Table S1) were synthesized by Eurofins Ltd Company (Melbourne, Australia). The relative expression level was presented relative to that of the corresponding control sample

at the indicated time, after normalization to actin transcript levels. All experiments were repeated three times.

Statistical analysis

Values presented are means ± either standard deviation (SD) or standard error (SE). Data were subjected to analysis of variance (ANOVA), and mean values were compared by Duncan's and Tukey's multiple range test ($P<0.05$). All statistical analysis was performed using SPSS 19.0 for Windows.

Results

Plants' ability to produce GABA alters their sensitivity to saline stress

In Arabidopsis, the gene *POP2* encodes GABA-T, which degrades GABA. The *pop2* mutant is unable to produce a functional GABA-T enzyme. As a result, the GABA content in roots of the *pop2-5* line was significantly higher (over 3-fold) than that in wild-type Columbia (Col) (Fig. 1A). GAD catalyses the conversion of glutamate to GABA; only a small difference (not significant at $P<0.05$) in GABA content was found between WT and *gad1,2* plants under control conditions. However, when the seedlings were subjected to NaCl stress, the GABA content in both Col and *pop2-5* roots was significantly increased (about 4-fold at the highest 100 mM NaCl treatment) while it remained largely unchanged in *gad1,2* roots. Regardless of the salt concentration used, the GABA content was several-fold higher in *pop2-5* compared with WT (Fig. 1A). This NaCl-induced increase in GABA concentration in roots was rapid and detected within 15 min of stress onset (Fig. 1B).

We then tested the sensitivity of various growth parameters to NaCl. A Petri dish experiments showed that under saline conditions the germination ability of *gad1,2* was reduced distinctly (Fig. 2A–D). Without NaCl, the fresh weight and root length were nearly the same in Col, *pop2-5*, and *gad1,2* seedlings. With the increase of NaCl concentration, both these characteristics were reduced (Fig. 2E–J). This salinity-induced inhibition of plant growth was most pronounced in *gad1,2* plants lacking an ability to respond to salt stress by increasing GABA levels. Similar trends were revealed for plants grown in soil (Fig. 3), where plants were exposed to salinity for the longer period, and plants were actively transpiring thus bringing the salt to the shoot. No difference was found in the shoot fresh and dry weight, chlorophyll content (SPAD value) and F_v/F_m among Col, *pop2-5*, and *gad1,2* under control condition. However, under salt treatment, *pop2-5* showed a salt-tolerant phenotype, having higher shoot fresh and dry weight, SPAD value and F_v/F_m compared with Col, whereas the *gad1,2* mutant showed a tendency to higher sensitivity (Fig. 3).

The ability of GABA-accumulating plants to develop a salt-tolerant phenotype when grown under saline conditions was further confirmed in experiments using two additional mutant lines (*pop2* and *gad1*; Supplementary Fig. S3). Also, supplying exogenous GABA was able to rescue salt-sensitive *gad1,2* phenotype (see Supplementary Fig. S4).

Ionic relations in Col, pop2-5, and gad1,2 mutants under salt stress

Because the different growth responses to NaCl treatment reported in Figs 2 and 3 may result from difference in their ability to prevent accumulation of Na^+ in the shoot, we tested this hypothesis. As shown in Fig. 4, the leaf sap Na^+ concentration was not different between Col and mutant plants under control condition, while under 50 and 100 mM NaCl treatments, the Na^+ content was significantly higher in *gad1,2* than that in Col and reduced in *pop2-5*. On the contrary, when subjected to salt stress, *pop2-5* accumulated considerably more K^+ in leaf than did *gad1,2* and Col, though there was no difference between Col and *gad1,2* (Fig. 4). These difference in Na^+ and K^+ content resulted in a substantially lower Na^+/K^+ ratio in *pop2-5* under salt stress, compared with both WT and *gad1,2* (Fig. 4C).

Elevated GABA levels improve root cell viability under conditions of oxidative and saline stress

Salinity stress results in a rapid accumulation of reactive oxygen species in plant roots, in a time-dependent and tissue-specific manner (Miller *et al.*, 2010; Nguyen *et al.*, 2017). Accordingly, we have quantified effects of salinity on H_2O_2 production in

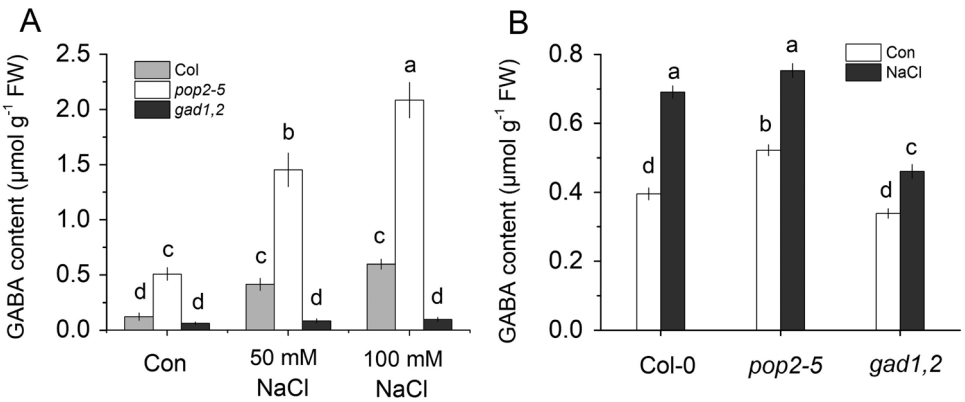

Fig. 1. GABA content in the roots of Arabidopsis Col-0, *pop2-5*, and *gad1,2* seedlings. (A) Arabidopsis seeds were sown in half-strength MS medium with 2% w/v phytogel infused with different salt concentrations in Petri dishes and grown for 7 d. (B) Plants were first grown in Petri dishes for 1 week in half-strength MS medium with 2% w/v phytogel and then transferred into quarter-strength Hoagland nutrient solution for 3 weeks. Seedlings were then treated with or without 100 mM NaCl for 15 min. Data are mean ±SD (n=3). Data labelled with different lowercase letters are significantly different at $P<0.05$ level.

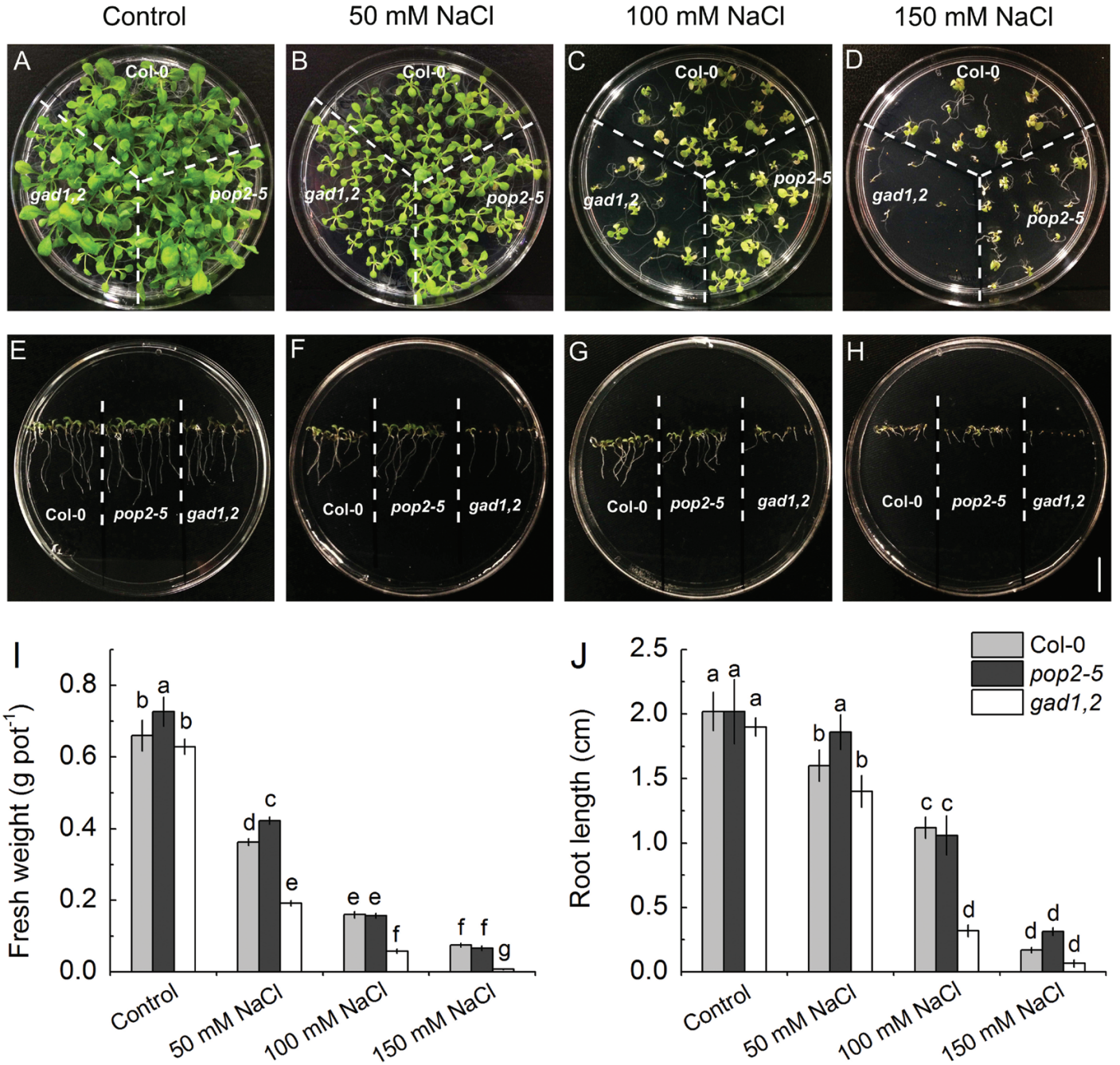

Fig. 2. Effects of NaCl stress on the morphology (A–H), fresh weight (I), and root length (J) of Arabidopsis Col, *pop2-5*, and *gad1,2* plants. (A–D) Plants were grown in Petri dishes for 3 weeks in half-strength MS medium with 2% w/v phytogel infused with different salt concentrations. The seedlings were photographed and the fresh weight was measured (I). (E–H) Root length of Col, *pop2-5*, and *gad1,2* Arabidopsis plants grown in vertically oriented Petri dishes for 1 week. Data are mean ±SD (n=5). Data labelled with different lowercase letters are significantly different at P<0.05 level. (This figure is available in color at *JXB* online.)

Arabidopsis roots at different times after stress exposure using two different methods. *In vivo* detection using fluorescent dye imaging revealed a biphasic response in H_2O_2 production, with two peaks observed at 2 and 12 h (Fig. 5A, B). Here, the H_2O_2 production was highest in *gad1,2* and lowest in *pop2-1*, suggesting a possible causal link between the amount of accumulated GABA and NaCl-induced reactive oxygen species (ROS) production in plant roots. These results were fully consistent with *in vitro* quantification of amount of accumulated H_2O_2 (Fig. 5C). Here, root H_2O_2 content increased about 4-fold (from ~0.05 to ~0.2 mmol g^{-1} FW) within 12 h of salinity treatment, with *pop2-5* plants showing significantly lower H_2O_2 levels compared with two other lines.

Both salinity and oxidative stress affect root cell viability (Jayakannan *et al.*, 2015). Accordingly, 4-day-old Arabidopsis seedlings were exposed to either 100 mM NaCl or 10 mM H_2O_2 treatments for 2 h, and then double stained with a fluorescein diacetate–propidium iodide dyes (Fig. 6A). Under the fluorescence microscope, viable cells fluoresced bright green, whereas dead or damaged cells fluoresced bright red. No dead

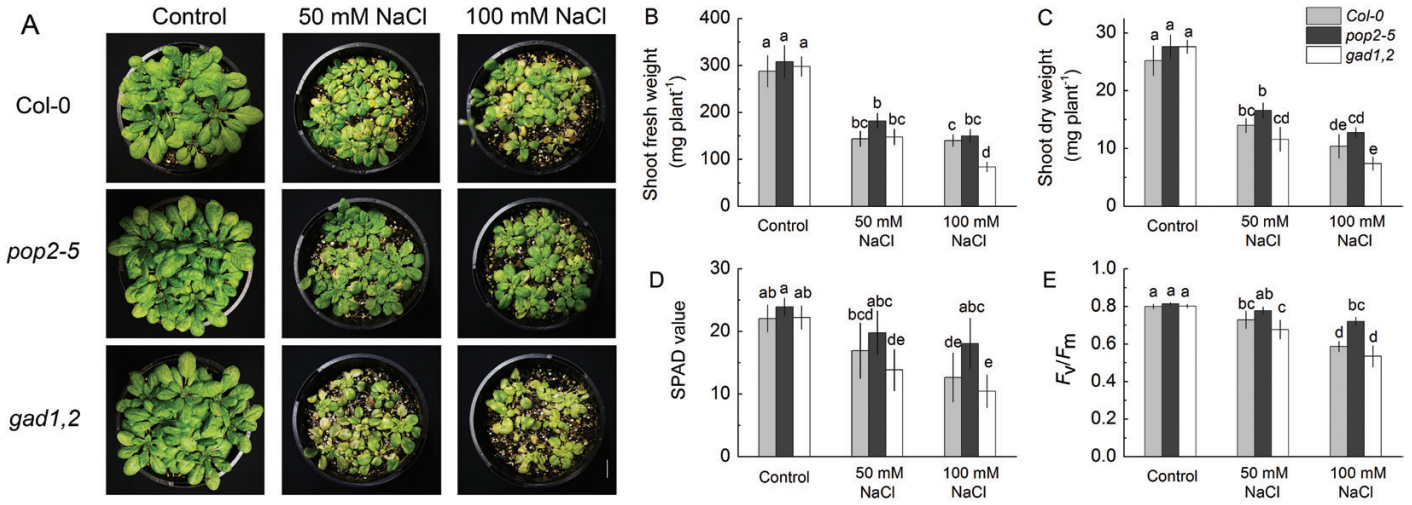

Fig. 3. Effects of salinity on morphology (A), shoot fresh weight (B), shoot dry weight (C), chlorophyll content (SPAD value; D), and chlorophyll fluorescence (F_v/F_m; E) of Arabidopsis Col, *pop2-5*, and *gad1,2* plants grown at various NaCl levels. All seedlings were grown in pots for 4 weeks under control conditions, followed by 2 weeks of salinity treatment. Data are mean ±SE (n=6). Data labelled with different lowercase letters are significantly different at P<0.05 level. (This figure is available in color at *JXB* online.)

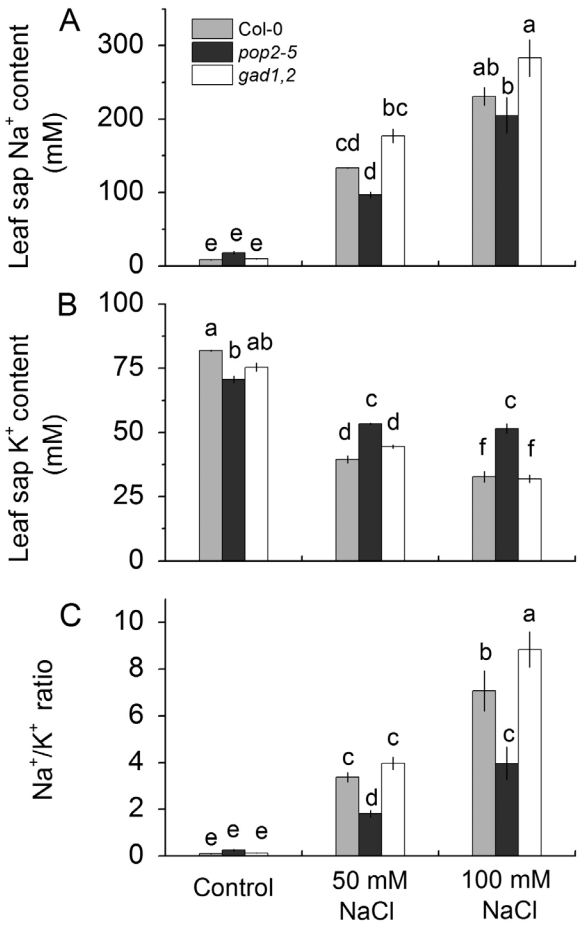

Fig. 4. The leaf sap Na^+ (A) and K^+ (B) content and shoot Na^+/K^+ ratio (C) of Arabidopsis Col, *pop2-5*, and *gad1,2* plants grown at various NaCl levels for 2 weeks. Salinity stress was applied to 4-week-old pot-grown plants. Data are mean ±SE (n=6). Data labelled with different lowercase letters are significantly different at P<0.05 level.

or damaged cells were found in the root tips in either line without NaCl treatment. Salinity exposure for 2 h resulted in a loss of cell viability in the root apex (less green signal), with *gad1,2* roots being affected most. The bright red signal appeared when the roots were treated with H_2O_2 for 2 h; this signal was strongest in WT and *gad1,2* roots, and was absent in *pop2-5* seedlings (Fig. 6A). The root viability was also measured by the TTC method. As shown in Fig. 6B, under all conditions *pop2-5* plants possessed the highest root viability. Two hours of NaCl treatment induced a decrease in a root viability only in *gad1,2*, with no changes observed in Col and *pop2-5*. While H_2O_2 inhibited root viability in all three lines; still the *pop2-5* line performed best of the three lines.

Higher GABA content results in the optimal Na^+/K^+ ratio in the root apex under saline stress conditions

The non-invasive microelectrode MIFE technique was further used to measure kinetics of NaCl-induced fluxes of K^+, H^+, and Na^+ in the roots of Arabidopsis GABA mutants. Addition of 100 mM NaCl to the bath induced a massive efflux of K^+, both in the elongation (Fig. 7A) and mature (Fig. 7B) root zones. Responses from the elongation zone were 4-fold stronger, indicating their higher sensitive to salinity. The peak K^+ efflux followed the trend *pop2-5*<WT<*gad1,2* (Fig. 7A) indicating a possible causal link with the level of endogenous GABA accumulated in roots. The difference in steady-state K^+ flux was significant (at P<0.05) in the elongation but not the mature root zone, 30 min after stress onset (see insets in Fig. 7A, B). Salinity treatment also shifted H^+ flux towards net efflux (in both zones; Fig. 7C, D). This shift was smallest in the *gad1,2* mutant. As a result, 30 min after salinity exposure, net H^+ efflux was measured in the *pop2-5* mutant in both zones while *gad1,2* roots showed net H^+ uptake (Fig. 7C, D). Responses in WT Col plants were in between. NaCl addition also caused a significant transient increase in the net Na^+ influx in all genotypes in both elongation and mature zones. The peak value of Na^+ influx in *gad1,2* was nearly 2-fold higher than that in *pop2-5*, with Col plants in between (Fig. 7E, F). The steady state Na^+ uptake was statistically different in plant

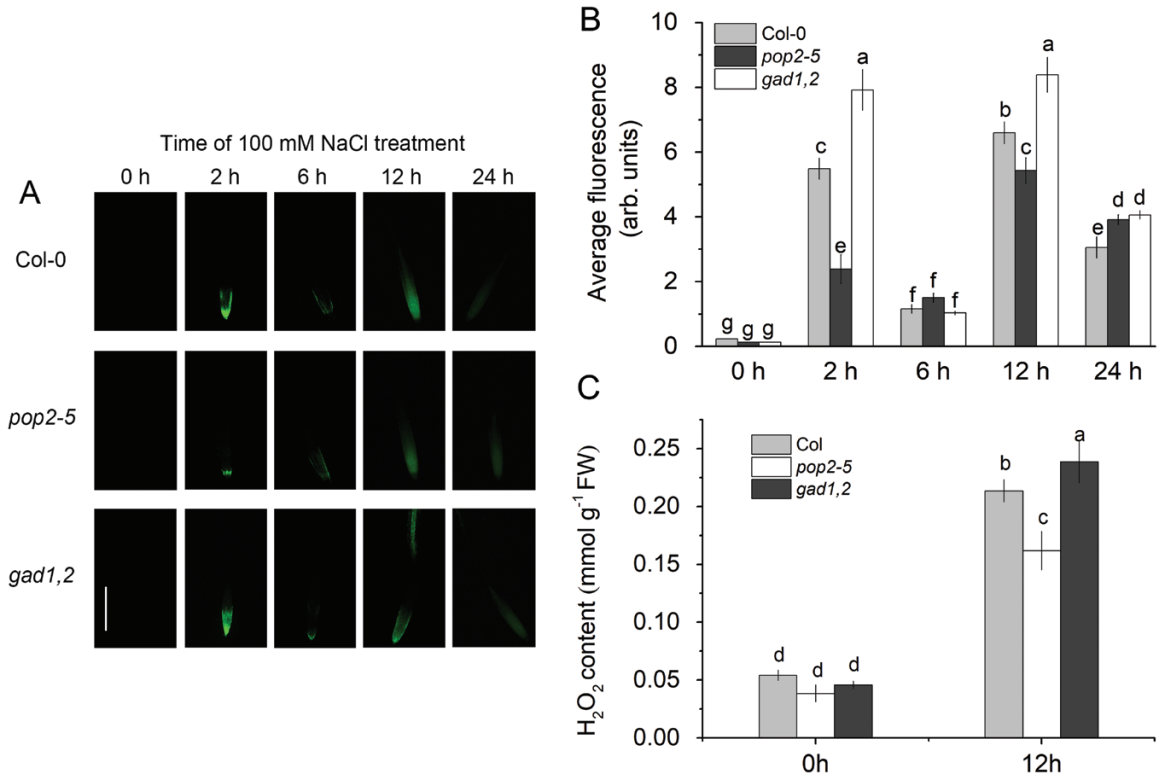

Fig. 5. Detection of H_2O_2 production in the roots *in vivo* (A, B) and *in vitro* (C) of Col-0, *pop2-5*, and *gad1,2* seedlings. (A, B) Four-day-old seedlings were treated with 100 mM NaCl for different time (0–24 h). Root samples were stained with 2′,7′-dichlorofluorescein diacetate for imaging under a fluorescence microscope. (A) Representative images. (B) Mean fluorescence intensity from elongation zone. (C) *In vitro* quantification of root H_2O_2 content at two time points by $TiCl_4$ method. Plants were first grown in Petri dishes for 1 week in half-strength MS medium with 2% w/v phytogel and then transferred into quarter-strength Hoagland nutrient solution for 3 weeks. Seedlings were then treated with or without 100 mM NaCl for 12 h. Data are mean ±SE (n=6). Data labelled with different lowercase letters are significantly different at P<0.05 level.

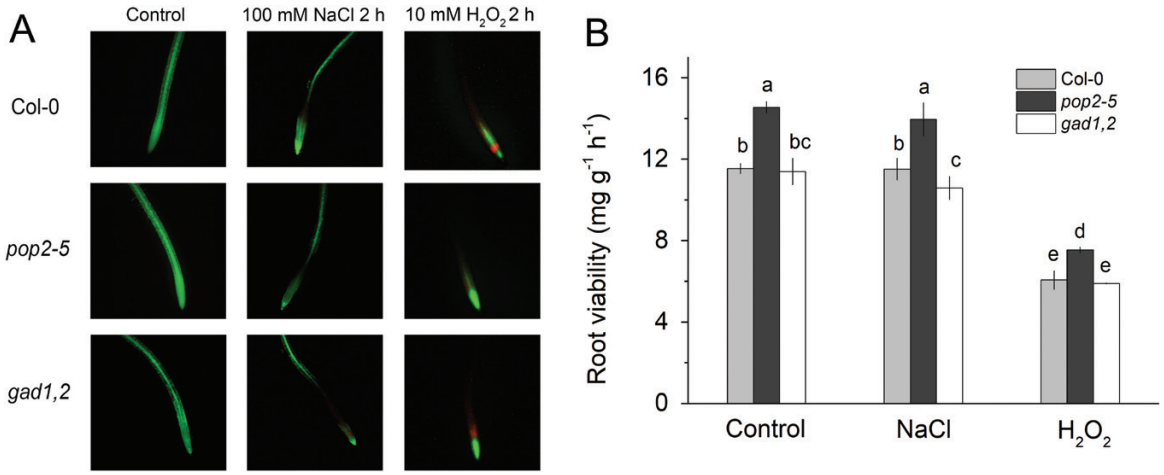

Fig. 6. Viability staining (A) and quantification (B) of Arabidopsis Col-0, *pop2-5*, and *gad1,2* roots. (A) Four-day-old plants were treated with either 100 mM NaCl or 10 mM H_2O_2 for 2 h and then double stained with fluorescein diacetate–propidium iodide for imaging under a fluorescence microscope. One (of six) typical images is shown for each treatment. (B) Root viability quantified by TTC method. Arabidopsis seedlings were cultivated in quarter-strength Hoagland solution for 4 weeks and then roots were treated with 100 mM NaCl or 10 mM H_2O_2 for 2 h. Data are mean ±SD (n=3). Data labelled with different lowercase letters are significantly different at P<0.05 level.

roots after 30 min of exposure (*pop2-5*<WT<*gad1,2*) both in the elongation and in the mature zones (Fig. 7E, F). The above observations obtained for *pop2-5* and *gad1,2* lines were further confirmed in experiments using two additional mutant lines (*pop2* and *gad1*). As shown in Supplementary Fig. S5, for NaCl-induced K^+ loss from the elongation zone, *pop2*<WT<*gad1*, while the opposite trend was observed for net Na^+ uptake (see Supplementary Fig. S5). Taken together, these results indicate that the differential ability of Arabidopsis plants to produce GABA has strongly affected plant ionic relations in the elongation root zone, with

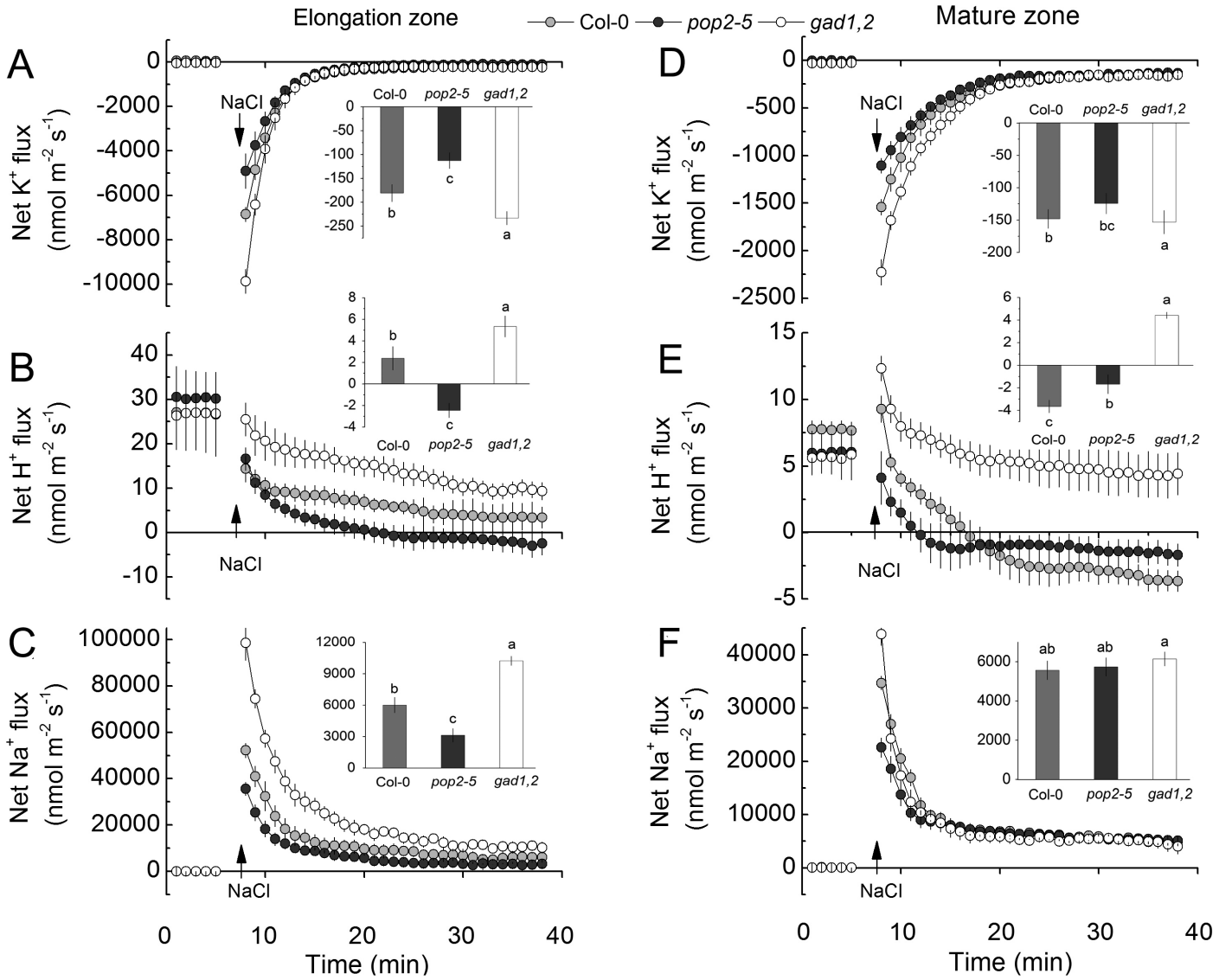

Fig. 7. Transient K^+, H^+ and Na^+ fluxes measured from the elongation zone (A–C) and mature (D–F) root zone of 4-day-old Col, *pop2-5*, and *gad1,2* seedlings in response to 100 mM NaCl treatment. The insets show steady fluxes after 30 min exposure to 100 mM NaCl. Data are mean ±SE (n=6). The sign convention is 'efflux negative'. Data labelled with different lowercase letters are significantly different at P<0.05 level.

plants producing more GABA being able to maintain a more optimal Na^+/K^+ ratio in the root apex.

H_2O_2-induced changes in net K^+ flux

As shown in Fig. 6, the three genotypes respond differently to H_2O_2 treatment. Thus, we measured H_2O_2-induced changes in K^+ flux. Similar to previous reports (Wang *et al.*, 2018), application of 10 mM H_2O_2 caused K^+ efflux from both the elongation and the mature zone of the root in all three Arabidopsis genotypes (Fig. 8). This H_2O_2-induced K^+ efflux was increased gradually over time, reaching peak values after 5–7 min of stress treatment. The K^+ efflux then gradually decreased but remained negative in the next 20 min. Compared with the response in the elongation zone, cells in the mature zone were less sensitive to H_2O_2 and exhibited a lower K^+ efflux level. Similarly, in both zones, the magnitude of K^+ efflux was the lowest in *pop2-5* and the highest in *gad1,2*, and they followed the sequence *gad1,2*>WT>*pop2-5*.

GABA-overproducing pop2-5 *plants maintain more negative membrane potential values in root epidermis when exposed to salinity*

Next the effect of NaCl on membrane potential in the different lines was analysed. The resting membrane potential in the elongation and mature zones in the three genotypes was nearly the same, approximately −100 mV, with no clear differences noted. NaCl addition induced a quick depolarization in a pronounced genotype-specific manner. The maximum depolarization was observed in *gad1,2*, especially in the elongation zone, followed by Col and then by *pop2-5*. The latter showed a minimum depolarization in both zones (Fig. 9A, B).

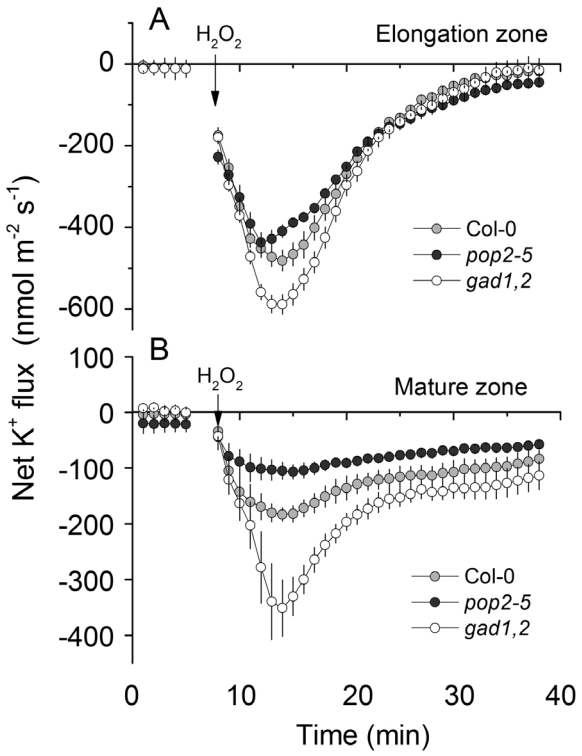

Fig. 8. Transient K^+ fluxes measured from the elongation (A) and mature (B) root zones of the 4-day-old Col, *pop2-5*, and *gad1,2* seedlings in response to acute 10 mM H_2O_2 treatment. Data are mean ±SE (n=6). The sign convention is 'efflux negative'.

In plant systems, membrane potential is maintained primarily by operation of the plasma membrane-based H^+-ATPase. In both WT and *pop2-5* mutant, the measured NaCl-induced shift towards H^+ efflux was completely suppressed by vanadate (Fig. 9C) suggesting that GABA operates upstream of H^+-ATPase.

Stress-induced transcriptional changes

The relative expressions of the key genes mediating cellular K^+ and Na^+ homeostasis were compared between the three genotypes. This included genes encoding: outward-rectifying K^+ efflux channels (*GORK* and *SKOR*); Na^+/H^+ exchangers (*SOS1* and *NHX1*); H^+-ATPase (*AHA2*); and ROS production (*RBOHF*). Under control condition, the expression of these genes in Col, *pop2-5*, and *gad1,2* did not show any significant difference (at P<0.05), while NaCl treatment up-regulated their transcription levels by different magnitudes (Fig. 10). The expression of *GORK* was significantly up-regulated by NaCl treatment in all three types, but it was nearly 3-fold higher in *gad1,2* than in Col and *pop2-5* (Fig. 10A). After salt treatment, the transcription of *SKOR* was increased particularly in Col and *gad1,2*, but was decreased in *pop2-5* (Fig. 10B). The expression levels of *NHX1*, *SOS1*, and *AHA2* showed the same trend, with *pop2-5* plants showing the highest increase followed by Col upon salinity exposure, while *gad1,2* showed only a modest increase (Fig. 10C–E). The *RBOHF* transcription level was up-regulated by NaCl treatment in all types, with *pop2-5* being least responsive (Fig. 10F).

Discussion

Higher GABA accumulation results in salt-tolerant phenotype

As expected, the *pop2-5* mutant accumulated more GABA in the roots (more than 2-fold under control and 3–4-fold upon salt stress than Col), and the GAD-deficient mutant *gad1,2* accumulated much less GABA, which even could not be induced by NaCl (Fig. 1A). As a result, the difference in the GABA content between these two mutants was about 20-fold in plants exposed to the highest salinity level used (Fig. 1A). This difference in the endogenous GABA content was reflected in differential sensitivity to salinity stress, with *pop2-5* having a salt-tolerant and *gad1,2* a salt-sensitive phenotype (Figs 2–4). These findings are in contrast to the results from Renault *et al.* (2010), in which *pop2-1* was oversensitive to salt tress. The reason for this discrepancy is not clear. One of the obvious differences is that those authors used Arabidopsis Ler ecoptype while our work was in the Columbia background. Also, the GABA content in their *pop2-1* mutant roots exposed to salinity treatment was more than 40 μmol g^{-1} DW (Renault *et al.*, 2010), while in our experiments the reported numbers were 2-fold lower (2 μmol g^{-1} FW, or 20 μmol g^{-1} DW, under 100 mM NaCl; Fig. 1A). Therefore, one possible explanation for this discrepancy may be that GABA may efficiently operate only in a certain concentration 'window', similar to that reported for other growth regulators such as polyamines (Pandolfi *et al.*, 2010). If the endogenous GABA concentration exceeds a certain threshold, deleterious or pleiotropic effects may be observed. Also, in their work Renault *et al.* (2010) used only one knock-out GABA-overproducing line, while our study used the *gad1,2* mutant with a lost ability for GABA biosynthesis, which showed increased sensitivity to NaCl.

Moreover, our results are also in a good agreement with reports that the *gad1,2* mutant is more sensitive to drought stress compared with WT (Mekonnen *et al.*, 2016) and that GABA priming improved osmotic stress tolerance in *Piper nigrum* (Vijayakumari and Puthur, 2016) and creeping bentgrass (*Agrostis stolonifera*; Li *et al.*, 2017). Given the fact that salinity is often called a 'physiological drought', these and our data suggest that the work by Renault *et al.* (2010) is an exception from the general trend, and that higher GABA levels are beneficial for salinity stress tolerance in plants.

GABA improves salinity stress tolerance by conferring optimal Na^+/K^+ ratio in plant tissues

Maintaining cellular ion homeostasis is an important adaptive trait of glycophytes under salt stress (Munns and Tester, 2008; Yang and Guo, 2018), with higher intracellular K^+/Na^+ ratios being associated with higher salinity stress tolerance (Yue *et al.*, 2012). When Arabidopsis seedlings were subjected to NaCl stress, the highest Na^+ and lowest K^+ contents were detected in the leaves of *gad1,2*; the opposite trend was found for *pop2-5* seedlings. As a result, the leaf sap Na^+/K^+ ratio was *gad1,2*,>WT>*pop2-5* (Fig. 4), correlating with the amount of GABA accumulated in plant tissues (Fig. 1).

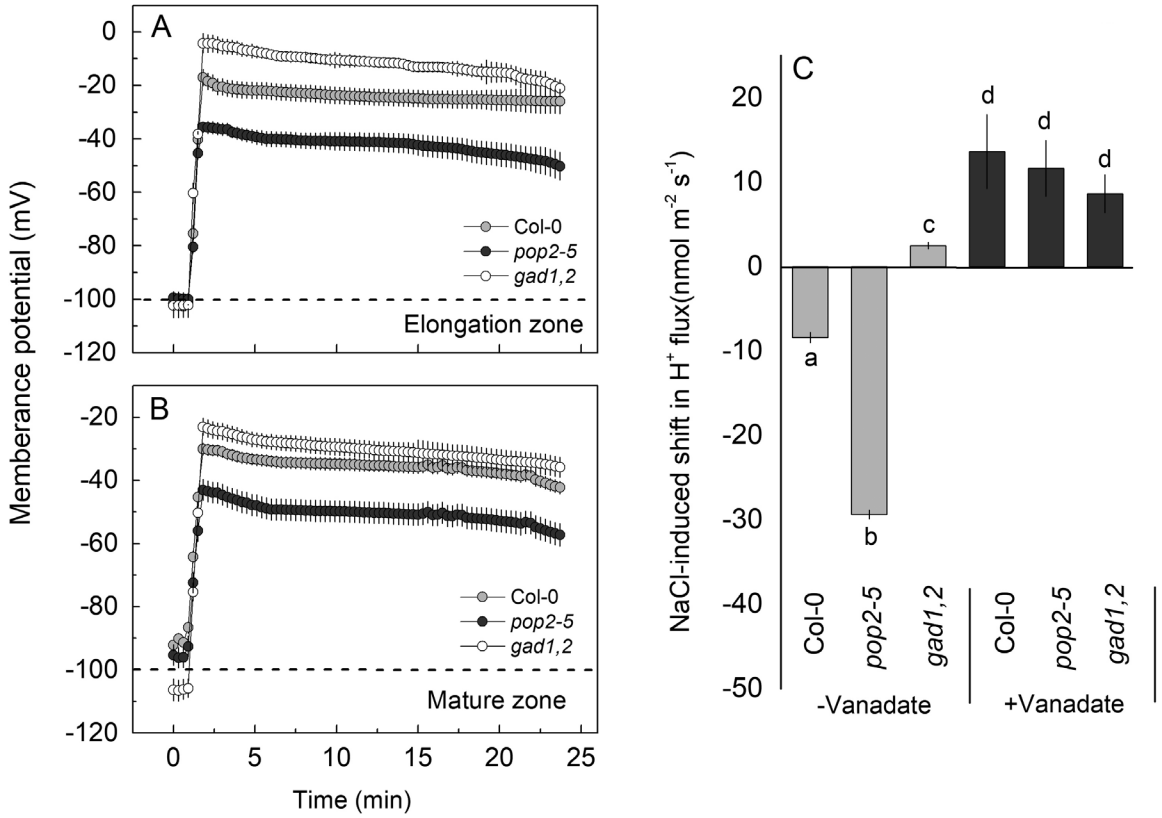

Fig. 9. (A, B) Salinity-induced changes in the plasma membrane potential in roots of 4-day-old Col-0, *pop2-5*, and *gad1,2* seedlings. Membrane potential was measured in the elongation (A) and mature (B) root zones of plants exposed to 100 mM NaCl. (C) Effect of the H^+-ATPase inhibitor sodium orthovanadate (Van) on the shift in net H^+ fluxes induced by NaCl measured from mature root zone. Light grey bars: changes in net H^+ fluxes from roots without sodium orthovanadate treatment; dark grey bars: changes in net H^+ flux values from roots with sodium orthovanadate pre-treatment. Data are mean ±SE (n=5).

The lower Na^+ accumulation in the shoots may be due to several factors including (i) lower net Na^+ uptake by roots; (ii) reduced rate of Na^+ transport to the shoot; and (iii) stronger Na^+ retrieval from the shoot (Munns and Tester 2008; Jayakannan *et al.*, 2015). To provide insights into this process, the transient net Na^+ flux was measured from plant roots upon salinity exposure. The magnitude of net Na^+ uptake in *gad1,2* was more than 2-fold that in *pop2-5* (Fig. 7E, F), explaining the difference in tissue Na^+ content.

When the Na^+ is absorbed and transported into shoots, the capability of excluding Na^+ from cytoplasm to apoplast and partitioning vacuolar Na^+ into the vacuole becomes a primary adaptive mechanism for reducing cytoplasmic ion toxicity in plants grown under high salt concentration (Hasegawa *et al.*, 2000). The plasma membrane Na^+/H^+ antiporter SOS1 is a key determinant of Na^+ transport from the cytoplasm to the apoplast (Shi *et al.*, 2000). The SOS1 operation is driven by the proton gradient created by the plasma membrane H^+-ATPase encoded by the *AHA* genes. The vacuolar Na^+ compartmentalization is mediated by the vacuolar Na^+/H^+ exchanger (NHX1) (Brini and Masmoudi, 2012), and a constitutive overexpression of *AtNHX1* and its orthologs in Arabidopsis led to increased plant salinity tolerance (Apse *et al.*, 1999). Here, we observed that under salt stress, the expressions of *SOS1*, *NHX1* and *AHA2* in roots were all up-regulated in the *pop2-5* mutant with elevated GABA content (Fig. 10). At the same time, *gad1,2* showed little increase in the transcription levels of *NHX1* and *AHA2*, and *SOS1* transcript levels barely changed (Fig. 10C–E). These results are consistent with the scenario that the salt-tolerant *pop2-5* mutant had an enhanced ability to reduce accumulation of cytotoxic Na^+ through two concurrent mechanisms. One is a superior Na^+ exclusion to the apoplast by SOS1, fueled by the higher plasma membrane H^+-ATPase activity. Supporting this notion is our observation of smaller net Na^+ uptake in plant roots and more negative H^+ flux values (indicating a higher rate of H^+-ATPase operation) in the GABA-overproducing *pop2-5* mutant. The second mechanism may include better Na^+ compartmentation into the vacuole (conferred by a higher level of NHX transcripts). All these features were lost (less functional) in the salt-oversensitive *gad1,2* mutant.

The mechanisms by which GABA levels control expression and activity of *SOS1* and *NHX1* genes remains to be determined. It was shown previously that GABA acts as a signaling molecule during drought stress by binding to GABA receptors (ALMT proteins) and also modulates the activity of H^+-ATPase via 14-3-3 proteins, thereby regulating stomatal movement (Mekonnen *et al.*, 2016). Given the fact that SOS1 is relieved from auto-inhibition upon phosphorylation of the auto-inhibitory domain by the SOS2–SOS3 kinase complex (Quintero *et al.*, 2011), the phosphorylation model of GABA regulation of SOS1 and NHX1 operation is plausible.

Another way of achieving a more optimal cytosolic Na^+/K^+ ratio is to increase tissue K^+ content. In this context, cytosolic

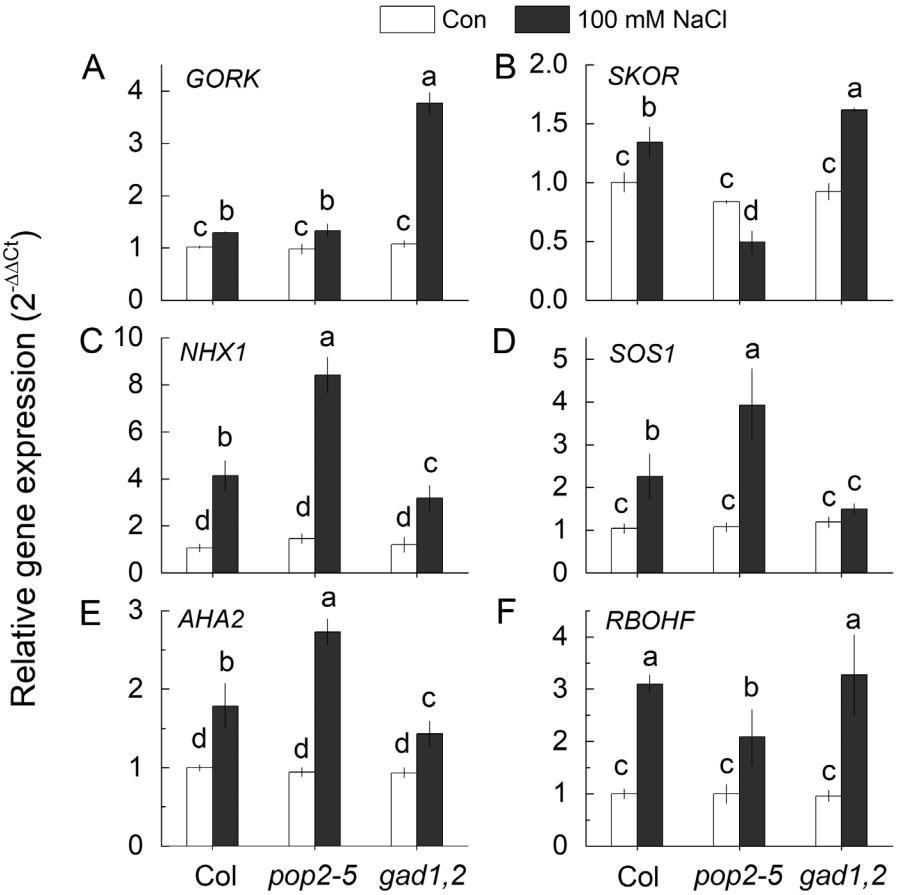

Fig. 10. Relative gene expression of *GORK*, *SKOR*, *NHX1*, *SOS1*, *AHA2*, and *RBOHF* in the roots of 4-week-old Col-0, *pop2-5*, and *gad1,2* seedlings under control and saline conditions. Plants were first grown in Petri dishes for 1 week in half-strength MS medium with 2% w/v phytogel and then transferred into quarter-strength Hoagland nutrient solution for 3 weeks. Seedlings were then treated with 100 mM NaCl for 12 h under standard condition (day/night cycle, 16/8 h; light intensity 100–150 mmol m^{-2} s^{-1}; temperature day/night, 25/20 °C). Data are mean values of three independent experiments with each containing three replicates. Data labelled with different lowercase letters are significantly different at $P<0.05$ level.

K^+ retention under salt stress is now firmly established as a key trait associated with salinity stress tolerance (Shabala and Cuin, 2008; Wu *et al.*, 2015; Shabala *et al.*, 2016). Under saline conditions, the massive entry of the positively charged Na^+ ions cause dramatic depolarization of the plasma membrane (Fig. 9A, B). Salt-tolerant genotypes typically show intrinsically more negative membrane potential values compared with their salt-sensitive counterparts (Chen *et al.*, 2007a; Smethurst *et al.*, 2008). Consistent with this, the root membrane potential of *pop2-5* was depolarized by about 60 mV, while this depolarization was nearly 100 mV in *gad1,2*, in the elongation zone. Also obvious was the difference in membrane potential depolarization between *pop2-5* and *gad1,2* in the mature zone (Fig. 9A, B).

In higher plants, the plasma membrane H^+-ATPase is considered to be a major contributor to the maintenance of the membrane potential (Palmgren and Nissen, 2011). Here we showed that NaCl treatment shifted H^+ fluxes towards net H^+ efflux in both zones. This shift was much stronger in *pop2-5* then in *gad1,2* (Fig. 7C, E), and was prevented by vanadate, a known inhibitor of the H^+-ATPase (Fig. 9C), indicating the involvement of the H^+-ATPase as a downstream target of GABA signaling. The substantial NaCl-induced depolarization reported here (Fig. 9A, B) resulted in an immediate K^+ leak via depolarization-activated outward rectifying K^+ GORK (AT5G37500) channels, as shown in experiments with knock-out *gork* lines (Shabala and Cuin, 2008). The reported difference in membrane potential values between *gad1,2* and *pop2-5* lines (about 30 mM less negative in salt-sensitive *gad1,2*; Fig. 9A, B) may explain a 2-fold higher K^+ efflux in this genotype. A stronger depolarization in the elongation zone may also explain a higher extent of K^+ efflux in this tissue. The process was further exacerbated by NaCl-induced upregulation of *GORK* transcript levels (Fig. 10A). This upregulation was only 30% in the salt-tolerant *pop2-5* but nearly 4-fold in the salt-sensitive *gad1,2*.

GABA accumulation mitigates salt stress through ROS pathway

Differential GABA accumulation in plant roots also affected roots' sensitivity to ROS, as indicated by both viability staining (Fig. 6) and the extent of sensitivity of K^+ transport systems to H_2O_2 (Fig. 8). The role of ROS in plant signaling and adaptation to salinity stress (as well as other stresses) is not straightforward. Low ROS concentrations can function as a signal that activate salt-stress responses, while high ROS concentrations damage proteins, lipids, DNA, and carbohydrates (Miller *et al.*, 2010). Amongst other sources, apoplastic ROS production by NADPH oxidase is considered to be a major source of

salt-stress-induced increase in ROS levels in plant roots (Kaye *et al.*, 2011; Bose *et al.*, 2014; Ben Rejeb *et al.*, 2015). In plants, NADPH oxidase is encoded by *Rboh/Nox* genes (Marino *et al.*, 2012; Morales *et al.*, 2016). Amongst 10 *Nox* genes in Arabidopsis, *RbohD* and *RbohF* are strongly up-regulated under salt stress (Ma *et al.*, 2012). Moreover, a *RbohF* mutant showed strong Na^+ hypersensitivity in its shoots (Jiang *et al.*, 2012). In our experiments, the amount of H_2O_2 in the roots of salt-tolerant *pop2-5* seedlings was minimal, while salt-sensitive *gad1,2* produced much more H_2O_2 than did *pop2-5* at 2 and 12 h after salt treatment (Fig. 5). Consistent with this, the expression of *RBOHF* in the shoot was also significantly higher in *gad1,2* compared with Col and *pop2-5* under salt stress (Fig. 10F), indicating that loss of GABA accumulation under salt stress resulted in more ROS production in both roots and shoots. This is in good agreement with reports by Shi *et al.* (2010) who showed that GABA treatment resulted in a lower NaCl-induced H_2O_2 production in the legume species *Caragana intermedia*.

Our previous experiments showed that higher H_2O_2-induced K^+ efflux in cereals, such as barley and wheat, correlated with their lower salinity tolerance (Chen *et al.*, 2007b; Maksimovic *et al.*, 2013; Wang *et al.*, 2018). Here we show that salt-tolerant *pop2-5* showed lowest K^+ leak when treated with H_2O_2, while the highest K^+ efflux was observed in the roots of the salt-sensitive *gad1,2* line (Fig. 8). Apoplastic H_2O_2 is known to interact with transition metals (Cu^{2+} and Fe^{2+}) in the cell wall, leading to formation of hydroxyl radicals (Demidchik, 2014). The latter were shown to be able directly activate GORK channels (Demidchik *et al.*, 2010), prompting massive K^+ efflux from Arabidopsis roots. In this context, stronger induction of net K^+ efflux by exogenous application of H_2O_2 in the salt-sensitive *gad1,2* line may be explained in several possible ways. First, these plants may possess intrinsically lower levels of endogenous antioxidants preventing hydroxyl radical formation. Second, the relative availability of Fe or Cu in the apoplast, or their reducing power, may differ between lines. Finally, there is the possibility of desensitization of GORK channels to $\cdot OH^-$. Future studies are required to differentiate between these possibilities.

Supplementary data

Supplementary data are available at *JXB* online.

Fig. S1. Relative gene expressions of *GAD1–GAD5* and *POP2* in the roots of 4-week-old Col-0, *pop 2-5*, and *gad1,2* seedlings.

Fig. S2. The homozygosis of *gad1* and *pop2*.

Fig. S3. Phenotypes of *pop2*, *gad1*, and Col-0 Arabidopsis seedlings treated with and without 100 mM NaCl.

Fig. S4. Exogenous GABA application rescues salt-sensitive *gad1,2* phenotype.

Fig. S5. Transient Na^+, K^+, and H^+ fluxes measured from the elongation zone and mature root zone of 4-day-old Col-0, *pop2*, and *gad1* seedlings in response to 100 mM NaCl treatment.

Table S1. The sequences of primers for qPCR.

Acknowledgements

This work was supported by National Natural Science Foundation of China (NSFC, No.31772360) to JC; Australian Research Council grant to SS; and funding from Foshan University to SS and MY. The co-first author QW was a recipient of China Scholarship Council (CSC). We thank M. Reichelt for support in GABA analysis.

References

Apse MP, Aharon GS, Snedden WA, Blumwald E. 1999. Salt tolerance conferred by overexpression of a vacuolar Na^+/H^+ antiport in *Arabidopsis*. Science **85**, 1256–1258.

Ben Rejeb K, Lefebvre-De Vos D, Le Disquet I, Leprince AS, Bordenave M, Maldiney R, Jdey A, Abdelly C, Savouré A. 2015. Hydrogen peroxide produced by NADPH oxidases increases proline accumulation during salt or mannitol stress in *Arabidopsis thaliana*. New Phytologist **208**, 1138–1148.

Bose J, Shabala L, Pottosin I, Zeng F, Velarde-Buendía AM, Massart A, Poschenrieder C, Hariadi Y, Shabala S. 2014. Kinetics of xylem loading, membrane potential maintenance, and sensitivity of K^+-permeable channels to reactive oxygen species: physiological traits that differentiate salinity tolerance between pea and barley. Plant, Cell & Environment **37**, 589–600.

Bose J, Xie Y, Shen W, Shabala S. 2013. Haem oxygenase modifies salinity tolerance in Arabidopsis by controlling K^+ retention via regulation of the plasma membrane H^+-ATPase and by altering SOS1 transcript levels in roots. Journal of Experimental Botany **64**, 471–481.

Bouché N, Fait A, Zik M, Fromm H. 2004. The root-specific glutamate decarboxylase (GAD1) is essential for sustaining GABA levels in *Arabidopsis*. Plant Molecular Biology **55**, 315–325.

Brini F, Masmoudi K. 2012. Ion transporters and abiotic stress tolerance in plants. ISRN Molecular Biology **3**, 927436.

Chen Z, Cuin TA, Zhou M, Twomey A, Naidu BP, Shabala S. 2007*a*. Compatible solute accumulation and stress-mitigating effects in barley genotypes contrasting in their salt tolerance. Journal of Experimental Botany **58**, 4245–4255.

Chen Z, Pottosin II, Cuin TA, *et al.* 2007*b*. Root plasma membrane transporters controlling K^+/Na^+ homeostasis in salt-stressed barley. Plant Physiology **145**, 1714–1725.

Clemensson-Lindell A. 1994. Triphenyltetrazolium chloride as an indicator of fine-root vitality and environmental stress in coniferous forest stands: Applications and limitations. Plant and Soil **159**, 297–300.

Cuin TA, Tian Y, Betts SA, Chalmandrier R, Shabala S. 2009. Ionic relations and osmotic adjustment in durum and bread wheat under saline conditions. Functional Plant Biology **36**, 1110–1119.

Demidchik V. 2014. Mechanisms and physiological roles of K^+ efflux from root cells. Journal of Plant Physiology **171**, 696–707.

Demidchik V, Cuin TA, Svistunenko D, Smith SJ, Miller AJ, Shabala S, Sokolik A, Yurin V. 2010. Arabidopsis root K^+-efflux conductance activated by hydroxyl radicals: single-channel properties, genetic basis and involvement in stress-induced cell death. Journal of Cell Science **123**, 1468–1479.

Fait A, Fromm H, Walter D, Galili G, Fernie AR. 2008. Highway or byway: the metabolic role of the GABA shunt in plants. Trends in Plant Science **13**, 14–19.

Hasegawa PM, Bressan RA, Zhu JK, Bohnert HJ. 2000. Plant cellular and molecular responses to high salinity. Annual Review of Plant Physiology and Plant Molecular Biology **51**, 463–499.

Hossain MA, Hasanuzzaman M, Fujita M. 2010. Up-regulation of antioxidant and glyoxalase systems by exogenous glycinebetaine and proline in mung bean confer tolerance to cadmium stress. Physiology and Molecular Biology of Plants **16**, 259–272.

Ismail AM, Horie T. 2017. Genomics, physiology, and molecular breeding approaches for improving salt tolerance. Annual Review of Plant Biology **68**, 405–434.

Jayakannan M, Bose J, Babourina O, Shabala S, Massart A, Poschenrieder C, Rengel Z. 2015. The NPR1-dependent salicylic acid signalling pathway is pivotal for enhanced salt and oxidative stress tolerance in Arabidopsis. Journal of Experimental Botany **66**, 1865–1875.

Jiang C, Belfield EJ, Mithani A, Visscher A, Ragoussis J, Mott R, Smith JA, Harberd NP. 2012. ROS-mediated vascular homeostatic control of root-to-shoot soil Na delivery in *Arabidopsis*. The EMBO Journal **31**, 4359–4370.

Kaye Y, Golani Y, Singer Y, Leshem Y, Cohen G, Ercetin M, Gillaspy G, Levine A. 2011. Inositol polyphosphate 5-phosphatase7 regulates the production of reactive oxygen species and salt tolerance in Arabidopsis. Plant Physiology **157**, 229–241.

Koyama H, Toda T, Yokota S, Zuraida D, Hara T. 1995. Effects of aluminium and pH on root growth and cell viability in *Arabidopsis thaliana* strain Landsberg in hydroponic culture. Plant and Cell Physiology **36**, 201–205.

Li Z, Yu J, Peng Y, Huang B. 2017. Metabolic pathways regulated by abscisic acid, salicylic acid and γ-aminobutyric acid in association with improved drought tolerance in creeping bentgrass (*Agrostis stolonifera*). Physiologia Plantarum **159**, 42–58.

Ma L, Zhang H, Sun L, Jiao Y, Zhang G, Miao C, Hao F. 2012. NADPH oxidase AtrbohD and AtrbohF function in ROS-dependent regulation of Na^+/K^+ homeostasis in Arabidopsis under salt stress. Journal of Experimental Botany **63**, 305–317.

Maksimovic JD, Zhang JY, Zeng FR, Zivanovic BD, Shabala L, Zhou MX, Shabala S. 2013. Linking oxidative and salinity stress tolerance in barley: Can root antioxidant enzyme activity be used as a measure of stress tolerance? Plant and Soil **365**, 141–155.

Marino D, Dunand C, Puppo A, Pauly N. 2012. A burst of plant NADPH oxidases. Trends in Plant Science **17**, 9–15.

Mekonnen DW, Flügge UI, Ludewig F. 2016. Gamma-aminobutyric acid depletion affects stomata closure and drought tolerance *of Arabidopsis thaliana*. Plant Science **245**, 25–34.

Miller G, Suzuki N, Ciftci-Yilmaz S, Mittler R. 2010. Reactive oxygen species homeostasis and signalling during drought and salinity stresses. Plant, Cell & Environment **33**, 453–467.

Miyashita Y, Good AG. 2008. Contribution of the GABA shunt to hypoxia-induced alanine accumulation in roots of *Arabidopsis thaliana*. Plant & Cell Physiology **49**, 92–102.

Morales J, Kadota Y, Zipfel C, Molina A, Torres MA. 2016. The Arabidopsis NADPH oxidases RbohD and RbohF display differential expression patterns and contributions during plant immunity. Journal of Experimental Botany **67**, 1663–1676.

Munns R, Tester M. 2008. Mechanisms of salinity tolerance. Annual Review of Plant Biology **59**, 651–681.

Nguyen HM, Sako K, Matsui A, Suzuki Y, Mostofa MG, Ha CV, Tanaka M, Tran LP, Habu Y, Seki M. 2017. Ethanol enhances high-salinity stress tolerance by detoxifying reactive oxygen species in *Arabidopsis thaliana* and rice. Frontiers in Plant Science **8**, 1001.

Palanivelu R, Brass L, Edlund AF, Preuss D. 2003. Pollen tube growth and guidance is regulated by *POP2*, an *Arabidopsis* gene that controls GABA levels. Cell **114**, 47–59.

Palmgren MG, Nissen P. 2011. P-type ATPases. Annual Review of Biophysics **40**, 243–266.

Pandolfi C, Pottosin I, Cuin T, Mancuso S, Shabala S. 2010. Specificity of polyamine effects on NaCl-induced ion flux kinetics and salt stress amelioration in plants. Plant & Cell Physiology **51**, 422–434.

Quintero FJ, Martinez-Atienza J, Villalta I, Jiang XY, Kim WY, Ali Z, Fujii H, Mendoza I, Yun DJ, Zhu JK, Pardo JM. 2011. Activation of the plasma membrane Na/H antiporter Salt-Overly-Sensitive 1 (SOS1) by phosphorylation of an auto-inhibitory C-terminal domain. Proceedings of the National Academy of Sciences, USA **108**, 2611–2616.

Ramesh SA, Tyerman SD, Gilliham M, Xu B. 2017. γ-Aminobutyric acid (GABA) signalling in plants. Cellular and Molecular Life Sciences **74**, 1577–1603.

Ramesh SA, Tyerman SD, Xu B, *et al.* 2015. GABA signalling modulates plant growth by directly regulating the activity of plant-specific anion transporters. Nature Communications **6**, 7879.

Renault H, El Amrani A, Berger A, Mouille G, Soubigou-Taconnat L, Bouchereau A, Deleu C. 2013. γ-Aminobutyric acid transaminase deficiency impairs central carbon metabolism and leads to cell wall defects during salt stress in Arabidopsis roots. Plant, Cell & Environment **36**, 1009–1018.

Renault H, Roussel V, El Amrani A, Arzel M, Renault D, Bouchereau A, Deleu C. 2010. The Arabidopsis *pop2-1* mutant reveals the involvement of GABA transaminase in salt stress tolerance. BMC Plant Biology **10**, 20.

Riccardi C, Nicoletti I. 2006. Analysis of apoptosis by propidium iodide staining and flow cytometry. Nature Protocols **1**, 1458–1461.

Rotman B, Papermaster BW. 1966. Membrane properties of living mammalian cells as studied by enzymatic hydrolysis of fluoregenic esters. Proceedings of the National Academy of Sciences, USA **55**, 134–141.

Scholz SS, Malabarba J, Reichelt M, Heyer M, Ludewig F, Mithöfer A. 2017. Evidence for GABA-induced systemic GABA accumulation in *Arabidopsis* upon wounding. Frontiers in Plant Science **8**, 388.

Scholz SS, Reichelt M, Mekonnen DW, Ludewig F, Mithöfer A. 2015. Insect herbivory-elicited GABA accumulation in plants is a wound-induced, direct, systemic, and jasmonate-independent defense response. Frontiers in Plant Science **6**, 1128.

Shabala L, Ross T, McMeekin T, Shabala S. 2006. Non-invasive microelectrode ion flux measurements to study adaptive responses of microorganisms to the environment. FEMS Microbiology Reviews **30**, 472–486.

Shabala S. 2013. Learning from halophytes: physiological basis and strategies to improve abiotic stress tolerance in crops. Annals of Botany **112**, 1209–1221.

Shabala S, Bose J, Fuglsang AT, Pottosin I. 2016. On a quest for stress tolerance genes: membrane transporters in sensing and adapting to hostile soils. Journal of Experimental Botany **67**, 1015–1031.

Shabala S, Bose J, Hedrich R. 2014. Salt bladders: do they matter? Trends in Plant Science **19**, 687–691.

Shabala S, Cuin TA. 2008. Potassium transport and plant salt tolerance. Physiologia Plantarum **133**, 651–669.

Shabala S, Shabala L. 2002. Kinetics of net H^+, Ca^{2+}, K^+, Na^+, NH_4^+, and Cl^- fluxes associated with post-chilling recovery of plasma membrane transporters in *Zea mays* leaf and root tissues. Physiologia Plantarum **114**, 47–56.

Shelp BJ, Mullen RT, Waller JC. 2012. Compartmentation of GABA metabolism raises intriguing questions. Trends in Plant Science **17**, 57–59.

Shi H, Ishitani M, Kim C, Zhu JK. 2000. The *Arabidopsis thaliana* salt tolerance gene *SOS1* encodes a putative Na^+/H^+ antiporter. Proceedings of the National Academy of Sciences, USA **97**, 6896–6901.

Shi SQ, Shi Z, Jiang ZP, Qi LW, Sun XM, Li CX, Liu JF, Xiao WF, Zhang SG. 2010. Effects of exogenous GABA on gene expression of *Caragana intermedia* roots under NaCl stress: regulatory roles for H_2O_2 and ethylene production. Plant, Cell & Environment **33**, 149–162.

Smethurst CF, Rix K, Garnett T, Auricht G, Bayart A, Lane P, Wilson SJ, Shabala S. 2008. Multiple traits associated with salt tolerance in lucerne: revealing the underlying cellular mechanisms. Functional Plant Biology **35**, 640–650.

Steward FC, Thompson JF, Dent CE. 1949. γ-Aminobutyric acid: a constituent of the potato tuber? Science **110**, 439–440.

Van Cauwenberghe OR, Makhmoudov A, McLean MD, Clark SM, Shelp BJ. 2002. Plant pyruvate-dependent gamma aminobutyrate transaminase: identification of an *Arabidopsis* cDNA and its expression in *Escherichia coli*. Canadian Journal of Botany **80**, 933–941.

Vijayakumari K, Puthur JT. 2016. γ-Aminobutyric acid (GABA) priming enhances the osmotic stress tolerance in *Piper nigrum* Linn. plants subjected to PEG-induced stress. Plant Growth Regulation **78**, 57–67.

Wang H, Shabala L, Zhou M, Shabala S. 2018, Hydrogen peroxide-induced root Ca^{2+} and K^+ fluxes correlate with salt tolerance in cereals: towards the cell-based phenotyping. International Journal of Molecular Sciences **19**, 702.

Widodo, Patterson JH, Newbigin E, Tester M, Bacic A, Roessner U. 2009. Metabolic responses to salt stress of barley (*Hordeum vulgare* L.) cultivars, Sahara and Clipper, which differ in salinity tolerance. Journal of Experimental Botany **60**, 4089–4103.

Wu H, Zhu M, Shabala L, Zhou M, Shabala S. 2015. K^+ retention in leaf mesophyll, an overlooked component of salinity tolerance mechanism: a case study for barley. Journal of Integrative Plant Biology **57**, 171–185.

Yang Y, Guo Y. 2018. Elucidating the molecular mechanisms mediating plant salt-stress responses. New Phytologist **217**, 523–539.

Yue Y, Zhang M, Zhang J, Duan L, Li Z. 2012. SOS1 gene overexpression increased salt tolerance in transgenic tobacco by maintaining a higher K^+/Na^+ ratio. Journal of Plant Physiology **169**, 255–261.

Zhang J, Zhang Y, Du Y, Chen S, Tang H. 2011. Dynamic metabonomic responses of tobacco (*Nicotiana tabacum*) plants to salt stress. Journal of Proteome Research **10**, 1904–1914.